Fabrication of hydrophobic structures on coronary stent surface based on direct three-beam laser interference lithography*

GAO Long-yue (高龙岳)[1], **ZHOU Wei-qi** (周玮琦)[1], **WANG Yuan-bo** (王渊博)[1], **WANG Si-qi** (王斯琦)[1], **BAI Chong** (白冲)[1], **LI Shi-ming** (李仕明)[1], **LIU Bin** (刘斌)[2], **WANG Jun-nan** (王珺楠)[2], **CUI Cheng-kun** (崔承坤)[1], **and LI Yong-liang** (李永亮)[1]**

1. School of Optoelectronic Engineering, Changchun University of Science and Technology, Changchun 130022, China

2. The Second Hospital of Jilin University, Changchun 130041, China

(Received 4 November 2015; Revised 4 February 2016)

To solve the problems with coronary stent implantation, coronary artery stent surface was directly modified by three-beam laser interference lithography through imitating the water-repellent surface of lotus leaf, and uniform micro-nano structures with the controllable period were fabricated. The morphological properties and contact angle (CA) of the microstructure were measured by scanning electron microscope (SEM) and CA system. The water repellency of stent was also evaluated by the contact and then separation between the water drop and the stent. The results show that the close-packed concave structure with the period of about 12 μm can be fabricated on the stent surface with special parameters (incident angle of 3°, laser energy density of 2.2 J·cm^{-2} and exposure time of 80 s) by using the three-beam laser at 1 064 nm, and the structure has good water repellency with CA of 120°.

Document code: A **Article ID:** 1673-1905(2016)03-0233-4

DOI 10.1007/s11801-016-6023-4

The coronary artery stent implantation has become the first choice for the treatment of coronary heart disease (CHD) in the world currently. Although the equipment and medication are increasingly improved, in-stent restenosis (ISR) is still a major defect of stent implantation[1]. Due to the occurrence of restenosis, still more than 15% patients with coronary stent implantation will accept interventional therapy in a year[2]. Therefore, it is of great significance to develop a new type of coronary stent, which has low restenosis rate and can prevent late stent thrombosis. In recent years, the studies show that the biocompatibility of the materials could be increased by the biomimetic process of surface and coating[3-8]. Consequently, the preparing bionic surface with regular geometric structure is beneficial to the rapid, directional and orderly adhesion and the growth of endothelial cells, which can reduce the formation of restenosis and late thrombosis.

Laser interference lithography (LIL) has been applied in many fields, such as solar cells[9,10], nano-scale patterned sapphire substrate[11] and bionics[12,13]. And studies have shown that the minimum feature size of direct LIL can reach 27 nm (laser wavelength of 308 nm, pulse width no more than 10 ns)[14], which can fully meet the requirements of the process in this paper. Compared with other approaches, such as electron beam lithography, ion beam lithography and scanning probe lithography, which adopt the point by point writing strategy[15,16], LIL reduces the required processing time by using multi-beam simultaneously. In addition, the long focal depth and the maskless process of LIL lower the flatness requirements of substrate and can realize imaging on a non-planar surface without affecting the resolution and image contrast.

In this paper, LIL is used to modify the surface of coronary stent by imitating the water-repellent surface of lotus leaf. Test results show that the processed stent has good water repellency, which can achieve the desired effects.

LIL is very suitable to process the coronary stent with the structure of mesh tubes, as shown in Fig.1. In the LIL method, the three-dimensional laser etching of materials was based on the energy distribution of multi-beam interference on the materials surface[15]. The intensity distribution pattern generated by interference is transferred to the material to produce periodic structures. By controlling the azimuthal angle, the polarization direction, the incident angle, the laser fluence, the exposure duration and other process parameters, we can utilize LIL

* This work has been supported by the National Natural Science Foundation of China (No.81470024).

** E-mail: liyongliang@cust.edu.cn

method to obtain micro-structures and nanostructures with particular size on the material surface[17].

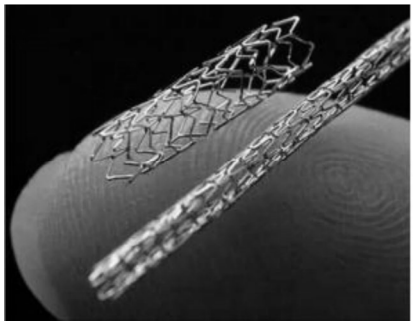

Fig.1 Photo of the compressed and expanded coronary artery stents

We can describe the three-beam interference with the superposition of electric field vectors of three laser beams, and it can be expressed as

$$\boldsymbol{E}=\sum_{i=1}^{3}\boldsymbol{E}_i=\sum_{i=1}^{3}A_i\boldsymbol{p}_i\cos(k\boldsymbol{n}_i\cdot\boldsymbol{r}_i\pm2\pi\omega t+\phi_i)\,, \tag{1}$$

and the interference intensity I can be calculated by

$$I=\left|\boldsymbol{E}\right|^2=\sum_{i=1}^{3}\sum_{j=1}^{3}A_i\boldsymbol{p}_i\cdot A_j\boldsymbol{p}_i\cos[k(\boldsymbol{n}_i\boldsymbol{r}_i-\boldsymbol{n}_j\boldsymbol{r}_j)]\,, \tag{2}$$

where A_i (i=1,2,3) is the amplitude, $\boldsymbol{p}_i$ (i=1,2,3) is the unit polarization vector, $k=2\pi\lambda^{-1}$ is the wave number, λ is the wavelength, $\boldsymbol{n}_i$ (i=1,2,3) is the position vector, and ϕ_i (i=1,2,3) is the phase constant. When three laser beams are configurated symmetrically with the same incident angles and the TE-TE-TM polarization mode, Eq.(2) can be simplified as

$$\begin{aligned}I_{\text{TE-TE-TM}}=A^2\{&3+2\cos(2kx\sin\theta)+\\&2\cos\left[2k(\frac{x}{2}+\frac{\sqrt{3}y}{2})\sin\theta\right]+\\&2\cos\left[2k(\frac{x}{2}-\frac{\sqrt{3}y}{2})\sin\theta\right]\},\end{aligned} \tag{3}$$

where θ is the incident angle, x and y are the coordinates, and $A_1=A_2=A_3=A$.

Fig.2 shows the two-dimensional and three-dimensional intensity distribution of the three-beam laser interference simulated by Matlab.

According to the theoretical analyses and computer simulations, the period of the interference pattern depends on the incident angle and the wavelength of laser beam, while the azimuthal angle also affects the period and the feature sizes of interference pattern[18]. And the critical feature sizes of the micro-structures and nanostructures are related to the laser fluence and the exposure time during the fabrication process. Besides, the model of pattern depends on the number of beams, for instance, grate and moth-eye structures are achieved by two-beam and six-beam laser interferences, respectively[13,19].

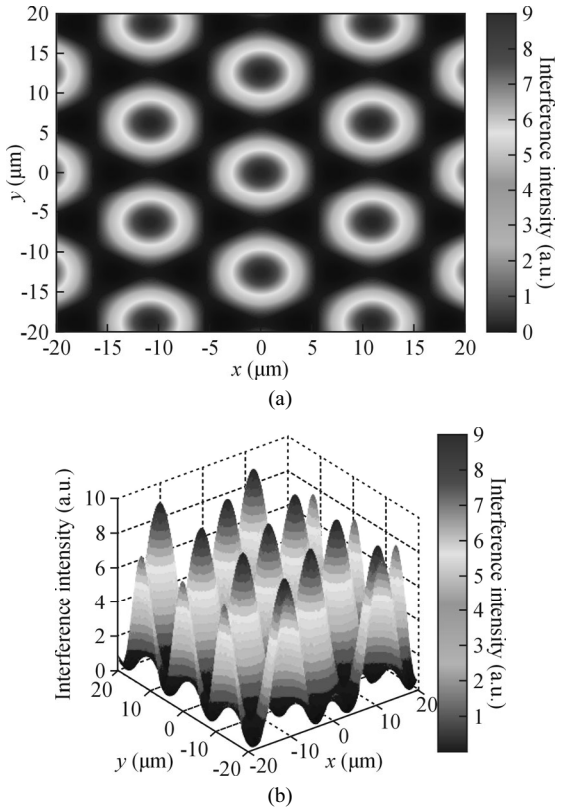

Fig.2 Simulation results of (a) two-dimensional and (b) three-dimensional intensity distribution of three-beam laser interference with the incident angle of 3° and the period of 12 μm

A three-beam interference system was built to produce the interference pattern for inducing concave structures on the stent surface. The structure is a direct consequence of the intensity modification[20]. Due to the high laser fluence, melt and evaporation behaviors of the laser ablation are the main mechanisms to modify the surface[19]. With the interaction of the laser beams, water-repellent structures can be created on the stent surface.

Baxter and Cassie[21] proposed the concept of composite contact during the study of water-repellent surface in nature. They think that the contact between the droplet and the rough surface is a kind of composite contact. Because the micro-structure scale of the surface is smaller than the droplet size, grooves on the rough surface cannot be filled with the droplets, and air is trapped under the liquid beads. So the contact surface between liquid and solid is composed of solid and gas[21], as shown in Fig.3. The contact angle (CA) of the composite surface can be expressed by the Cassie-Baxter equation as[21]

$$\cos\theta=f_1\cos\theta_1+f_2\cos\theta_2\,, \tag{4}$$

where θ_1 and θ_2 are the CAs of the flat solid and air surfaces, and f_1 and f_2 are the solid and air surface area fractions, respectively.

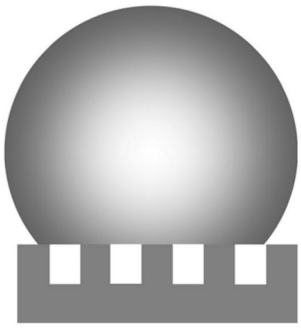

Fig.3 Typical Cassie-Baxter model for wetting behavior of a water droplet on the rough solid substrate

In the experiment, highly ordered hydrophobic structures were fabricated on the surface of the coronary stent by laser lithography technology based on three-beam interference. Coronary stent used in the experiment was made of stainless steel. The laser source was a solid-state high-power pulsed Nd:YAG laser with the wavelength of 1 064 nm, frequency of 10 Hz, pulse duration of 7 ns, pulse energy of 2 J and beam diameter of 9 mm. Quarter-wave plates and polarizers were placed before the exposed sample to control the energy and polarization of each beam. All the experimental results were obtained in the air.

Fig.4 shows the schematic diagram of a three-beam laser interference system. The laser beam passes through two beam splitters (BSs) and three high reflectivity mirrors, and then converges together to produce interference. The azimuthal angles of three laser beams are ϕ_1=0°, ϕ_2=120°, ϕ_3=240°, the incident angles are $\theta_1=\theta_2=\theta_3$=3°, and the polarization angles are set to be $\psi_1=\psi_2$=90°, ψ_3=0°.

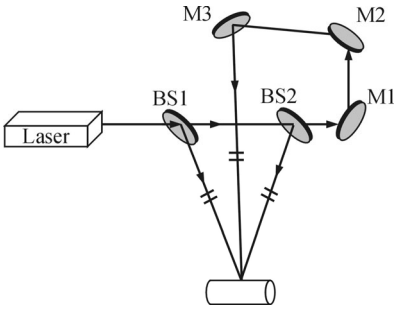

Fig.4 Schematic diagram of a three-beam laser interference system

Under the action of high power nanosecond laser, the stainless steel material melts and evaporates during the exposure process. Fig.5 shows the scanning electron microscope (SEM) images of the processed stent surface. The stent surface is covered by the concave structures, which largely improve the water-repellent capability. It can be seen from Fig.5(b) that the period of dots is about 12.194 μm, and it has a good agreement with the theoretical analyses shown in Fig.2.

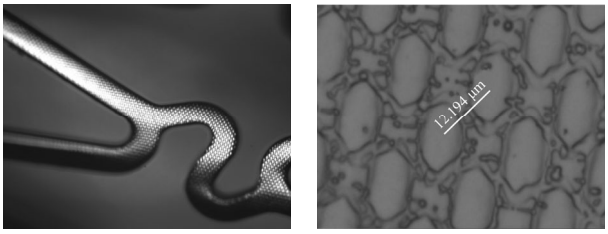

(a) (b)

Fig.5 (a) SEM images of the processed stent surface at low magnification; (b) Close-up image of concave structure at high magnification

The theoretical CA of a water drop can be calculated according Eq.(4). In Fig.5(b), the area of concave structure is about 520 μm^2, and the whole area is 803 μm^2.The result value of f_1 is 0.468. The water CA θ_1 of the untreated stent surface is about 90°. According to Eq.(4), the water CA is about 120.9°.

In the experiment, the laser energy density and exposure time both have huge impact on CA. By choosing reasonable parameters, the water-repellent surface can be obtained. Here, the laser energy density is 2.2 J·cm^{-2}, the exposure time is 80 s, and the final CA is 120°, as shown in Fig.6.

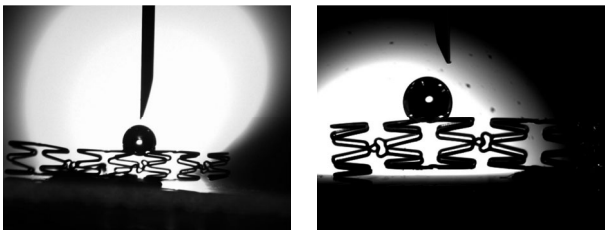

(a) (b)

Fig.6 Photos of a spherical water droplet (a) on the untreated stent surface with the corresponding water CA of 90°and (b) on the processed stent surface with the corresponding water CA of 120°

In addition to the measurement of CA, we also use another way to evaluate water-repellent capability of the processed stent surface, which is making the water droplet to contact with stent and then separate, meanwhile, observing stent surface adsorption of water droplet. Fig.7 shows the test procedure taken by high speed camera. We can see from Fig.7 that no water-drop remains on the surface of the processed stent, which means the water-repellent property of the stent is excellent.

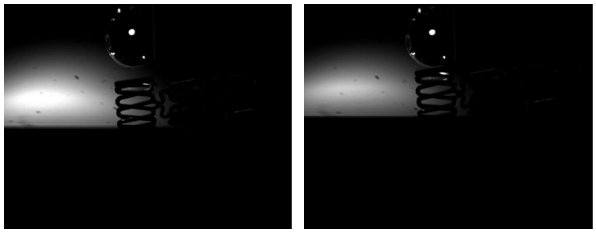

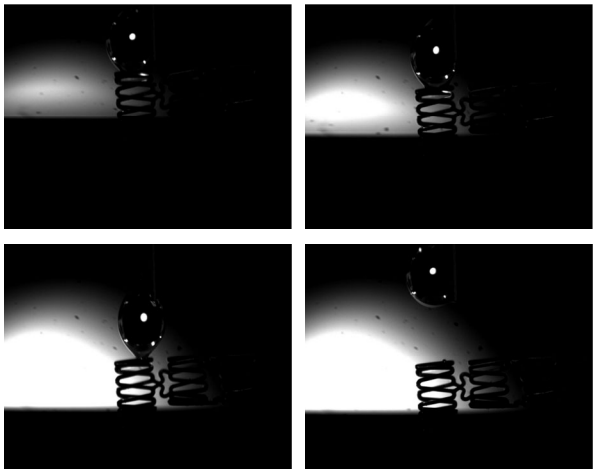

Fig.7 Process of contact and separation of water droplets from the stent

In this paper, stent surface is directly modified by LIL based on a three-beam laser interference system. By selecting the proper process parameters, highly ordered concave structures were fabricated with the period of 12 μm. Test results show that this kind of the micro-structures has a relative high CA and low water absorption capacity. The theoretical and experimental results show that the water-repellent property of the coronary stent is significantly improved, which can lay a foundation for new generation bionic coronary stent to solve the problem of restenosis and thrombosis.

References

[1] E. Camenzind, New England Journal of Medicine **355**, 2149 (2006).

[2] F. Alfonso, R. A. Byrne, F. Rivero and A. Kastrati, Journal of the American College of Cardiology **63**, 2659 (2014).

[3] Liu Ruiming, Qin Yuansen, Wang Huijin, Zhao Yong, Hu Zuojun and Wang Shenming, Bmc Cardiovascular Disorders **13**, 1 (2013).

[4] Feng Wang, Liang Shi, Wen-Xi Hea, Dong Hand, Yan Yana, Zhong-Ying Niu and Sheng-Gen Shi, Applied Surface Science **265**, 480 (2013).

[5] Liu Yan, Yin Xiaoming, Zhang Jijia, Wang Yaming, Han Zhiwu and Ren Luquan, Applied Surface Science **280**, 845 (2013).

[6] C. M. Han, H. E. Kim and Y. H. Koh, Surface & Coatings Technology **251**, 226 (2014).

[7] V. Leszczak and K. C. Popat, Acs Applied Materials & Interfaces **6**, 15913 (2014).

[8] C. K. Akkan, M. E. Hammadeh, A. May, H.-W. Park, H. Abdul-Khaliq, T. Strunskus and O. C. Aktas, Lasers in Medical Science **29**, 1633 (2014).

[9] S. Domínguez, O. García, M. Ezquer, M. J. Rodríguez, A. R. Lagunas, J. Pérez-Conde and J. Bravo, Photonics and Nanostructures - Fundamentals and Applications **10**, 46 (2012).

[10] K. S. Cho, P. Mandal, K. Kim, I. H. Baek, S. Lee, H. Lim, D. J. Cho, S. Kim, J. Lee and F. Rotermund, Optics Communications **284**, 2608 (2011).

[11] Xuan Ming-dong, Dai Long-gui, Jia Hai-qiang and Chen Hong, Optoelectronics Letters **10**, 51 (2014).

[12] ZHANG Hai-xin, CHEN Xu-lang, ZHANG Lu-jia, LIU Guang-ze, ZHANG Jin-jin, WANG Da-peng and WANG Zuo-bin, Journal of Optoelectronics · Laser **25**, 2283 (2014). (in Chinese)

[13] J. Xu, Z. Wang, Z. Zhang, D. Wang and Z. Weng, Journal of Applied Physics **115**, 203101 (2014).

[14] Fab New Laser Nano-Fabrication Technology, http:// phys.org / news / 2010-05-fab-laser-nano-fabrication-technology. html

[15] S. R. J. Brueck, Proceedings of the IEEE **93**, 1704 (2005).

[16] S. M. Lubin, W. Zhou, A. J. Hryn, M. D. Huntington and T. W. Odom, Nano Letters **12**, 4948 (2012).

[17] W. Li, Z. Wang, D. Wang, Z. Zhang, L. Zhao, D. Li, R. Qiu and C. R. Maple, Optical Engineering **53**, 1709 (2014).

[18] J. Zhang, Z. Wang, X. Di, L. Zhao and D. Wang, Applied optics **53**, 6294 (2014).

[19] D. Wang, Z. Wang, Z. Zhang, Y. Yue, D. Li and C. Maple, Applied Surface Science **282**, 67 (2013).

[20] T. Tavera, N. Pérez, A. Rodríguez, P. Yurrita, S. M. Olaizola and E. Castaño, Applied Surface Science **258**, 1175 (2011).

[21] A. B. D. Cassie and S. Baxter, Transactions of the Faraday Society **40**, 546 (1944).